

We are IntechOpen, the world's leading publisher of Open Access books Built by scientists, for scientists

6,900

Open access books available

186,000

International authors and editors

200M

Downloads

Our authors are among the

154

Countries delivered to

TOP 1%

most cited scientists

12.2%

Contributors from top 500 universities



WEB OF SCIENCE™

Selection of our books indexed in the Book Citation Index
in Web of Science™ Core Collection (BKCI)

Interested in publishing with us?
Contact book.department@intechopen.com

Numbers displayed above are based on latest data collected.
For more information visit www.intechopen.com



The Emerging Field Trends Erosion-Free Electric Hall Thrusters Systems

*Iryna Litovko, Alexey Goncharov, Andrew Dobrovolskyi
and Iryna Naiko*

Abstract

The Hall-type accelerator with closed Hall current and open (that is unbounded by metal or dielectric) walls was proposed and considered both theoretically and experimentally. The novelty of this accelerator is the use of a virtual parallel surface of the anode and the cathode due to the principle of equipotentialization of magnetic field lines, which allows to avoid sputtering of the cathode surface and preserve the dynamics of accelerated ions. The formation of the actual traction beam should be due to the acceleration of ions with the accumulated positive bulk charge. A two-dimensional hybrid model in cylindrical coordinates is created in the framework of which the possibility of creation a positive space charge at the system axes is shown. It is shown that the ions flow from the hump of electrical potential can lead to the creation of a powerful ion flow, which moves along the symmetry axis in both sides from the center.

Keywords: Hall thruster, accelerator with closed Hall current, plasmaoptical system, plasma lens, low temperature plasma, space charge, ion flow, crossed electric and magnetic fields

1. Introduction

The realization that outer space is becoming an integral part of our earthly existence becomes commonplace. Hundreds of all kinds of spacecraft (maneuverable and marching), plow the vastness of the vast space. The moving force of such spacecraft has become the electric propulsions different kinds. Traditionally, Hall thrusters (plasma accelerators with closed Hall current and metal or dielectric walls [1–4] attract a special attention of the electric propulsion community. Remarkably high efficiency, simplicity, and potential durability make the Hall thruster one of the primary candidates for miniaturization and application in small communications satellites and using for primary propulsion in deep-space scientific missions. Hall thrusters inherit coaxial geometry for which the material of the annular chamber walls significantly affects the plasma discharge properties and erosion of the dielectric walls. In order to avoid erosion developers, try to create modified wall less accelerator constructions [5, 6]. But these attempts while are not completed, quite complicated and sound many skepticisms.

One of the promising ways to avoid erosion issues is the separation of the magnetic and electrical circuits of the accelerator, which is easier to do in the cylindrical geometry. This principle was carried out and tested in the original Hall type erosion-less accelerator on a laboratory stand at the Institute of Physics NAS of Ukraine [7–10]. The novelty of the proposed idea is the use of a virtual parallel surface of the anode to the cathode due to the principle of equipotentialization of magnetic field lines. Which allows to avoid sputtering of the cathode surface. It was shown the potential drop forms at the axis of system that can use for ion beam formation and accelerating.

We describe the Hall-type accelerator with closed Hall current and open (that is unbounded by metal or dielectric) walls that was proposed and considered both theoretically and experimentally. A two-dimensional hybrid model in cylindrical coordinates is constructed in the framework of which the possibility of creation a positive space charge at the system axes is shown. It is shown that the ions flow from the hump of electrical potential can lead to the creation of a powerful ion flow, which moves along the symmetry axis in both sides from the center. The formation of the actual traction beam should occur due to the acceleration of ions by the accumulated positive bulk charge. Thus, such type of accelerator could sound interest in manipulating high-current flow of charge particle as well as can be attractive for many different high-tech applications and for potential elaborations of low cost, compact and durability electric thrusters.

This article is the brief review of the current status an ongoing experimental and theoretical research and simulations results of such kind accelerator based on the axial-symmetric cylindrical electrostatic plasma lens configuration and the fundamental plasma-optical principles of magnetic electron isolation and equipotentialization magnetic field lines.

2. Experimental setup and results

Experiments were carried out on a laboratory stand, the schematic diagram of which is shown in **Figure 1** on the left. Vacuum chamber 1 contained a test mockup of the accelerator with open walls. The accelerator consisted of a magnetic core with permanent magnets 2 and an electrode system with cylindrical anode 3 and cathode 4 formed by a system of pins. The experimental installation allowed a controlled gas input, by usinCHA-2 system. The gas pumping was performed with the use of a vacuum unit with an oil-vapor pump. The photo of the accelerator with anode layer and open wall is shown in **Figure 1** on the right.

As can be seen from the **Figure 1** on the left, the cathode is composed of two parts that are separated in space. The ends of the cathode pins coincide with the magnetic surfaces that in area between them are parallel to the anode surface. The application of the plasmaoptics principles to the design of a cylindrical accelerator with anode layer and open walls allowed to create an accelerator with virtual cathode that is parallel to the anode plane for its entire width and with cathode that is several centimeters wide. That allows to form a wide flow of accelerated ions to the system axis of symmetry. Due to that each part of the cathode is made in the form of pins, the collecting surface area is significantly reduced, that reduces the contribution of the cathode material in the flow.

The discharge in the system burns due to the working gas (argon) ionization by the electrons. Electrons are magnetized and formed stable negative space charge. The created ions are accelerated from the ionization zone towards the cathode.

The formation of the magnetic field is provided by a system of permanent magnets located in the magnetic circuit. By selecting the number and polarity of the

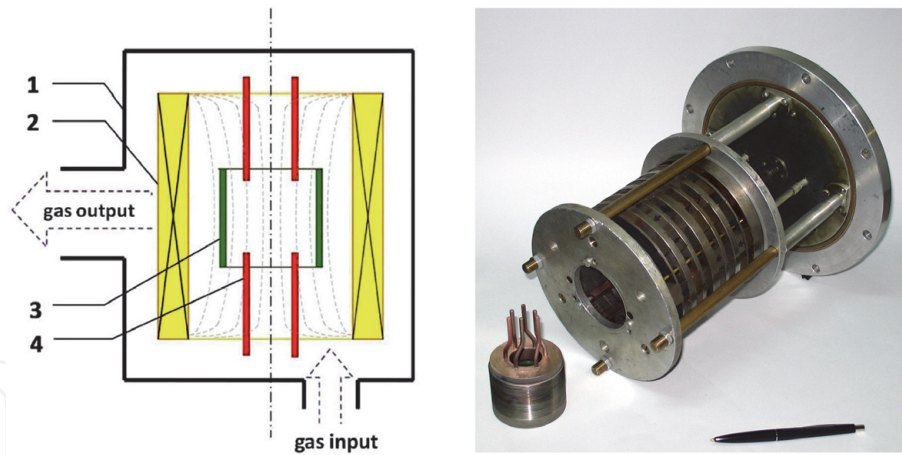


Figure 1.
Left: Experimental setup; vacuum chamber (1), magnetic system ($H= 650-750$ Oe) (2), anode (3), cathode (4). Right: Photo of the accelerator with anode layer and open walls.

magnets in each system layer, it was possible to change the magnetic field geometry in a wide range. In experiment the system of permanent magnets was arranged in such a way that the magnetic field in the gap between the cathode and the anode was parallel to system's axis as much as possible. It was owing to this configuration of the magnetic field that a system with open walls was created.

2.1 Experimental results

As mentioned above, the cathode is composed of two parts separated in space and their edge coincide with magnetic field lines that are parallel to anode surface. The magnitude of the magnetic field is such that Larmor radius of the electron is much smaller than the system radius. Due to this, the principle of the equipotentialization of magnetic field lines with accuracy up to the electron temperature works [11]. Accordingly, a cylindrical virtual surface is formed between these parts, which potential is close to cathode potential. Through the electrons drift in the crossed electric and magnetic field $E \times H$ there is a closed Hall current and corresponding space charge, that creates a layer near the anode surface where the main potential drop occurs [12]. With the appearance of the Hall current in the perpendicular direction, the electron current along E becomes small. In turn, the ions are almost unaffected by the magnetic field, because the Larmor radius of the ion is more than characteristic system size [2, 13]. Ions under the electric field influence, moving in the cathode direction, converge to the center and are pushed out of the system along the axis. The electrons exit speed from the system along the axis is quite small and is compensated by the working gas ionization by these electrons. At low pressure, ionization occurs between the anode and virtual cylindrical cathode. With increasing pressure, the anode layer size can reach the radius of the system. The operation modes of the accelerator also change [9].

The dependence of the current strength on the applied potential to the anode for different working gas pressure were obtained experimentally. The results of the effect of the change in the working gas pressure in the source volume on the discharge current density for the low-current mode are shown in the **Figure 2**. For the presented curves for different voltages, it can be seen that the current density little depends on the gas pressure in the system for potentials up to 1,5 kV in the discharge gap.

This result can be explained by the assumption that the ionized particles concentration under these conditions does not depend on the working gas pressure. This corresponds to the obtained theoretical results also.

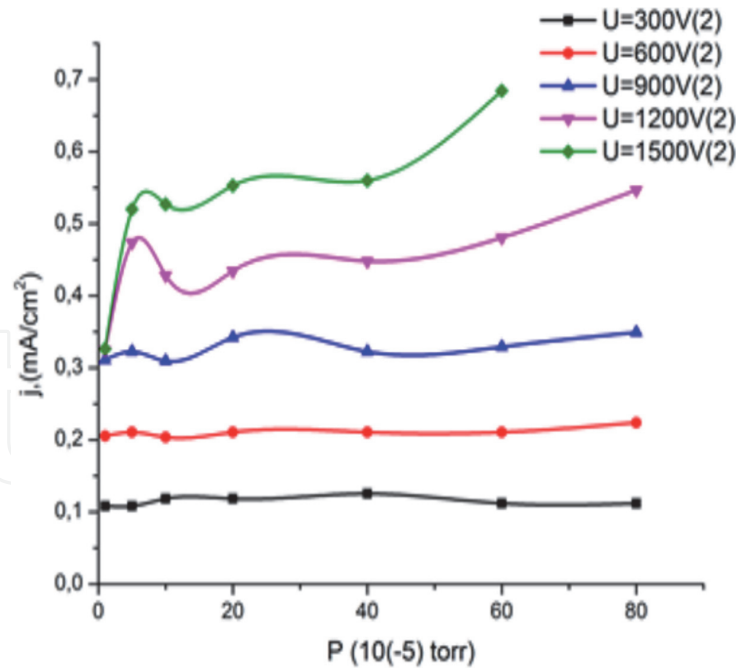


Figure 2. Dependence of current density on the pressure the chamber at different values of the voltage applied to the discharge gap.

Note that the operation modes of this kind accelerator are very close to those of the classical accelerator with an anode layer. There are two operation modes of this kind accelerator. The first is low-current, with a clearly visible narrow radiating layer between the anode and cathode, in the range of 10^{-4} Torr. The current increases monotonically with increasing applied voltage (see **Figure 3a**). With increasing pressure at a constant applied voltage, this layer gradually occupies the entire volume of the accelerator. During this mode, the ions are mostly formed in a narrow anode layer and move towards the system axis, hardly experiencing the influence of a magnetic field. Accumulating on the system axis, they are pushed out of the volume along it. The study of the distance changing influence between the virtual cathode and anode showed the existence of the optimum. The maximum current on the system axis is fixed at a distance $d=10$ mm between electrodes, as one can see from **Figure 3a**.

In the second mode – high current, the discharge extends to the entire internal system volume. When the voltage reached a certain value ($U > 1,8$ kV), the

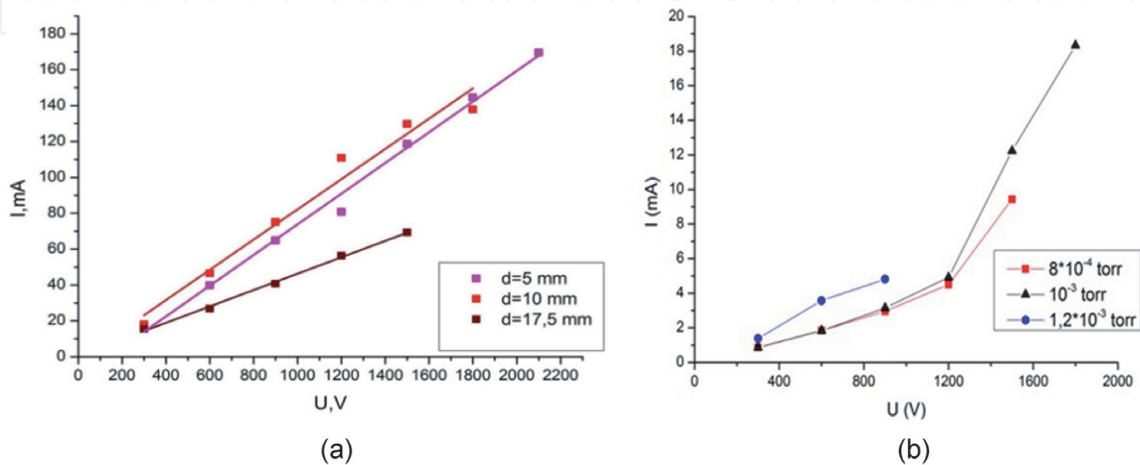


Figure 3. Volt-ampere characteristic of the accelerator in low-current mode at a) different distance between the anode and cathode at pressure 10^{-4} Torr and b) at different values of pressure in chamber.

discharge current increased in a jump-like manner (see **Figure 4a**), and the discharge transitioned into the high-current mode, in which the distinct anode layer was absent. In this mode, a typical discharge current was several orders of magnitude higher (up to 2 A, as can be seen from **Figure 4**) than in the low-current mode. Thus, It is evident that the transition into the high-current mode occurs under the influence of two factors: the working gas pressure (see **Figure 3b**) and the voltage applied across the discharge gap (**Figure 4**).

Another characteristic feature of the high-current mode is the formation of a plasma torch. At the discharge voltage $U > 1,8$ kV bright radiation is observed from the system volume from the ends of the cylindrical channel along the rotation symmetry axis (see **Figure 5a**). In the discharge concerned, ions are accelerated along system's radius towards system's axis. The torches at the ends, on the contrary, are observed along the axis, perpendicularly to the radius and the direction of initial ion acceleration.

Thus, owing to the discharge geometry, in space limited by electrodes of the accelerator there is an accumulation of ion space charge like a lens with a positive space charge, that was proposed earlier for negatively charged particles beam focusing [14–17]. The generated ions reach the system axis and accumulate in the region around it. Ions are stored in the cylinder volume until their own space charge creates a critical electric field. This field forces ions to leave the volume. The main part of the generated ions escapes from the system perpendicularly to its radius. Due to this plasma torches are formed at the edges of the device, which are clearly

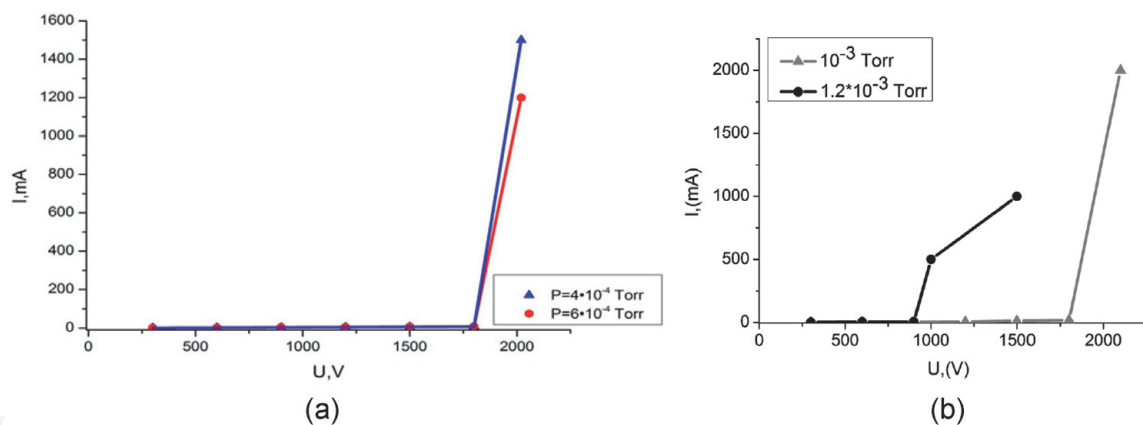


Figure 4. Volt-ampere characteristic of the accelerator at different pressure in a) low-current mode b) high-current mode.

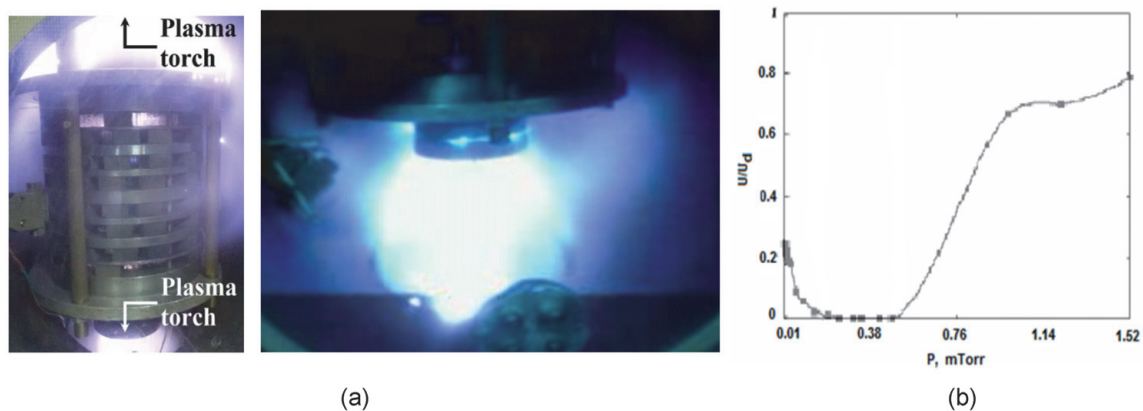


Figure 5. a) Plasma jet from volume of thruster in high current operation mode. b) Floating potential dependence on the pressure at the system edge.

visible in high-current mode. The results of measuring the floating potential along the axis of the system show that under certain conditions along the plasma torch axis there may be a potential drop (see **Figure 5b**), which can be used to accelerate the generated ions and form a charged particles beam.

Radial studies of the plasma flow coming out along the system axis in this device at different pressures revealed a significant increase in current density on the axis (see **Figure 6**). That fact may indicate the plasma acceleration in this direction. The study of the dependence of the uncompensated current density on the accelerator volume shows the existence of a maximum for a pressure of $6 \cdot 10^{-4}$ Torr. This operation mode of the accelerator is mostly interesting for use as a prototype of the ion-plasma small rocket engine.

Determination of the ion energy distribution function (see **Figure 7a**) in this accelerator was performed by retarding potential method using a 3-line analyzer (discharge current 1.5–2 A; voltage 1.5–2.1 kV; pressure in the range 10^{-4} – 10^{-3} Torr). The research results showed the formation of a sufficiently monoenergetic beam with of FWHM (as can be seen from **Figure 7b**), at the level of 10% of the average value which reached two thirds of the anode discharge potential (in particular, at $U_{\text{anode}} = 1.8$ kV, $E = 1.2$ keV).

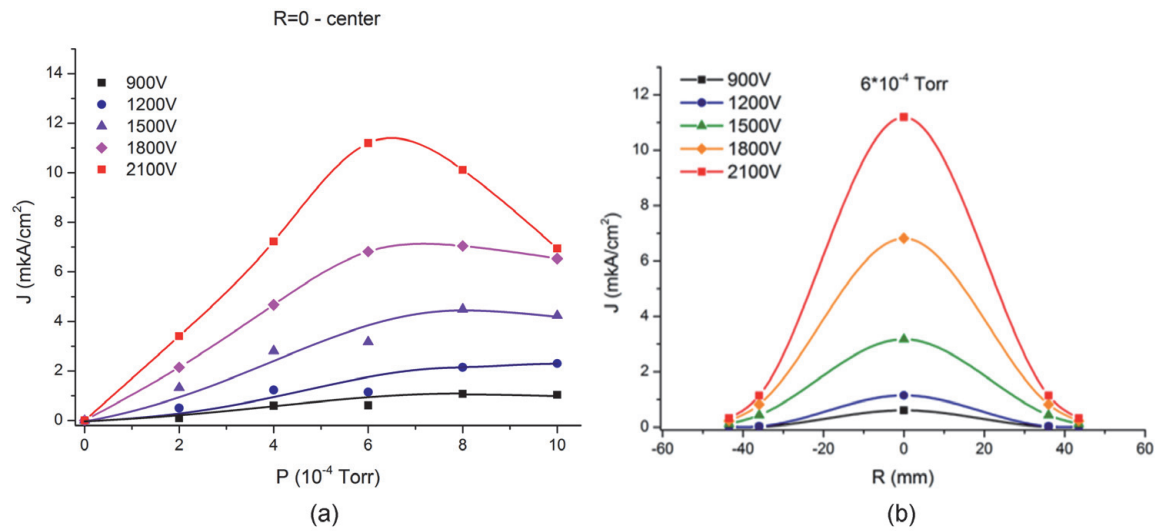


Figure 6. a) Distribution of the current density along the system radius at the accelerator output. b) the dependence of the current density on the system axis on the pressure in chamber at different values of potential at the anode.

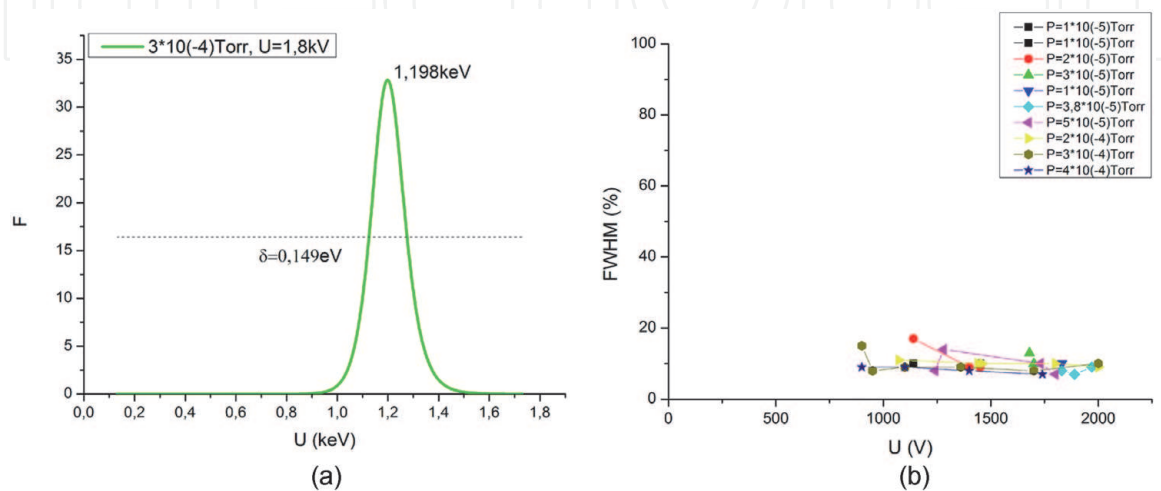


Figure 7. a) Ion energy distribution function ion energy distribution function (voltage 1.8 kV; pressure $3 \cdot 10^{-4}$ Torr). b) the dependence of FWHM (full width at half maximum) on the voltage applied to the anode.

3. Theoretical model

3.1 One-dimensional hydrodynamic and hybrid model

3.1.1 Hydrodynamic model

To clarify the obtained experimental data, primarily a one-dimensional hydrodynamical theoretical model was developed (see **Figure 8a**). Here x-axis is directed along the radius of the system. We have considered the discharge gap, where ions production appear due to working gas ionization by electrons. Electrons are magnetized, move along magnetic strength lines and drift slowly to anode due to collisions. Ions are free and accelerated by electric field move to the system axis.

The closed system of equations that describes such system in hydrodynamic approximation in stationary state has the form:

$$j_e + j_i = j_d \quad (1)$$

$$j_i(x) = e\nu_i \int_0^x n_e(x) dx \quad (2)$$

$$j_e(x) = e\mu_{\perp} \left(n_e E(x) - \frac{d}{dx} (n_e T_e) \right) \quad (3)$$

$$T_e(x) = \frac{\beta}{j_e(x)} \int_0^x j_e \frac{d\phi}{ds} ds \quad (4)$$

$$n_i(x) = \sqrt{\frac{M}{2e}} \int_0^x \frac{n_e(s) \nu_i ds}{\sqrt{\phi(x) - \phi(s)}} \quad (5)$$

$$n_e - n_i = \frac{1}{4\pi e} \phi'' \quad (6)$$

here j_i, j_e, n_i, n_e - are ion and electron current density and density consequently, ν_i - is the ionization frequency, $\mu_{\perp} = \frac{e\nu_e}{m\omega_{eH}^2}$ - electron transverse mobility, E - electric field: $E(x) = -\frac{d\phi}{dx}$, ϕ - potential, ν_e is the frequency of elastic collisions with neutrals and ions, ω_{eH} - the electron cyclotron frequency, T_e - electron temperature.

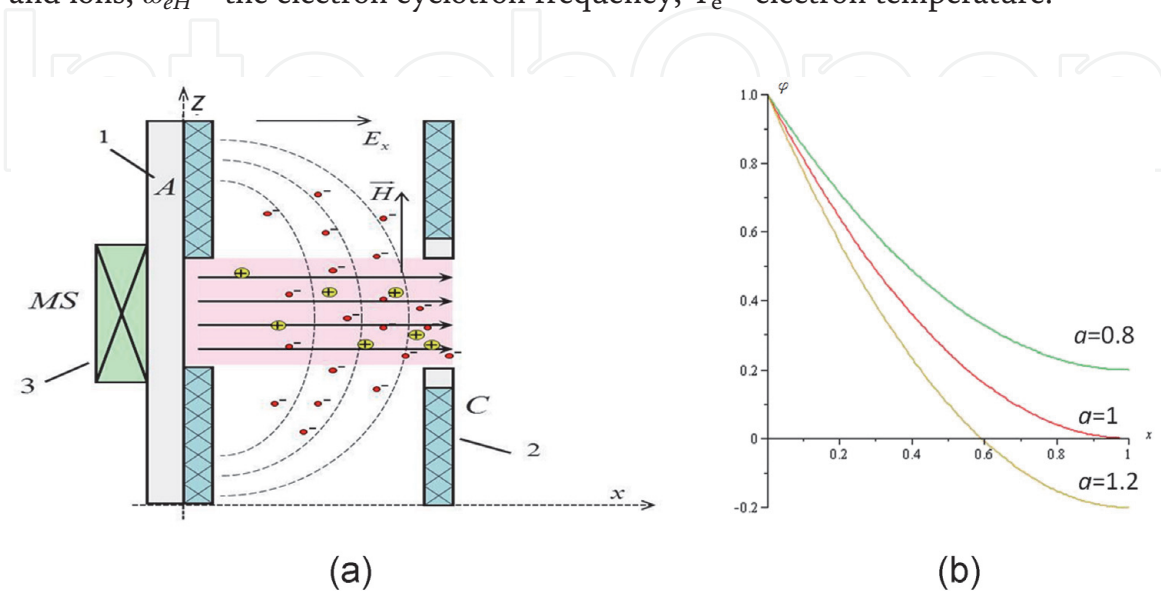


Figure 8.
 a) Model of discharge gap: 1- anode, 2- cathode, 3- permanent magnets system; b) potential distribution in the gap for different parameters α value.

In the framework of this model, both exact analytical and numerical solutions were obtained [7, 10]. Based on the idea of continuity of current transferring in the system and assumption that the discharge current density in gap volume is the sum of the ion and electron components are found exact analytical solutions describing electric potential distribution along acceleration gap, if $T_e = \text{const}$. It has the next form in low-current mode:

$$\phi = a \left((x - 1)^2 - 1 \right) + 1, \quad (7)$$

where a is parameter equals $a = \frac{\nu_i d^2}{2\mu_{\perp} \phi_a}$, d – gap length. The potential distribution in the gap for different value of the parameter a is present in **Figure 8b**. It is found under conditions when all electrons originated within the gap by impact ionization only and go out at the anode due to mobility in transverse magnetic field, the condition of full potential drop in the accelerating gap corresponds to equality gap length to the anode layer thickness. In case when the gap length is less than anode layer thickness, potential drop is not completed, and positive space charge dominated. For case when the gap length is more than anode layer, potential drop exceeds applied potential. This can be due to electron space charge dominated at the accelerator exit. It was shown that potential distribution is parabolic for different operation modes as in low-current mode well as in high current quasi neutral plasma mode and weakly depends on electron temperature. For high-current mode solution has form like expression (7):

$$\phi(x) = 1 + \frac{a^2}{2f^2} \left((x - 1)^2 - 1 \right) \quad (8)$$

where $f = \nu_i d \sqrt{\frac{M}{2e\phi_a}}$ – describes impact of ion density. Note, that if $a = 2f^2$ we obtain (7). This condition can be rewritten in form:

$$\frac{\tau_{ed}}{\tau_{id}^2} = 2\nu_i \text{ or } \tau_{ed}\nu_i = 2\tau_{id}^2\nu_i^2 = 1 \quad (9)$$

here $\tau_{ed} = \frac{d}{\mu_{\perp} E}$ – electron lifetime, $\tau_{id} = \frac{d}{v_{id}}$ – ion lifetime. Indeed (9), is some generalization condition of self-sustained discharge in crossed $E \times H$ fields taking into consideration both electron and ion dynamic peculiarities.

To clarify the effect of electron temperature on the characteristics of accelerating layer, it was assumed that the electrons received energy from the electric field, thus $T_e = \beta \cdot \phi$, where $0 < \beta \leq 1$. In this assumption, the solution has the form:

$$\phi(x) = \frac{a}{1 + \beta} x(x - 2) + 1 \quad (10)$$

Consider a more complete description, assuming that heat loss occurs due to different types of collision. Entering the characteristic time τ_0 – energy loss by collision, expression for electron temperature (4) can be represented as:

$$T_e = \frac{j_d E \tau_0}{en_e} \left(1 - e^{-t/\tau_0} \right) \quad (11)$$

If we assume that τ_0 is equal to electron lifetime τ_{ed} , we obtain:

$$T_e = \frac{j_d d}{\mu_{\perp} e n_e} \quad (12)$$

Thus, the second term in expression (3) disappears and we come back to the solution (7). The numerical solution of system Eq. (1)–(6) showed that the electron density changes extraordinarily little along the gap with typical operating parameters, so our assumption about $n_e = \text{const}$ is justified.

So, even in such a simplified model, we obtain a result explaining the appearance a space charge and finding the optimal length of accelerating gap. Nevertheless, although the hydrodynamic model can well describe the dynamics of the electron and ionic components, it does not make allowance for ionization state processes, as well as the influence of neutral atoms in the working gas. A purely kinetic description cannot also be used because of a significant difference between the velocities of electrons and ions. Therefore, a description using the hybrid model may be an optimal decision.

3.1.2 Hybrid model

In the framework of this model [18, 19], the hydrodynamic description is used for the electron component, and the kinetic description for the ionic and neutral ones. This approach also allows the limited stay time of ions in the system to be considered. A one-dimensional model was considered with regard for only the single ionization. In this case, we can write the following equations for neutrals and ions, respectively.

$$\frac{\partial f_0}{\partial t} + v_0 \frac{\partial f_0}{\partial x} = -\langle \sigma_{ie} v_e \rangle n_e f_0 \quad (13)$$

$$\frac{\partial f_i}{\partial t} + v_i \frac{\partial f_i}{\partial x} + \frac{e}{M} E \frac{\partial f_i}{\partial v} = \langle \sigma_{ie} v_e \rangle n_e f_0 \quad (14)$$

here f_0, f_i – distribution function of neutrals and ions consequently, that satisfy boundary conditions:

$$\begin{aligned} f_0(0, v, t) &= \frac{1}{(2\pi MT)^{\frac{3}{2}}} \exp\left(-\frac{Mv^2}{2T}\right), v > 0 \\ f_0(0, v, t) &= 0, v < 0; \\ f_i(0, v, t) &= 0 \end{aligned} \quad (15)$$

In (13) and (14) right part expression is:

$$\langle \sigma_{ie} v_e \rangle = \sigma_{\max} v_e(T_e) \exp\left(\frac{-U_i}{T_e}\right) \quad (16)$$

here σ_{\max} – maximal ionization cross-section, $v_e(T_e)$ – average electron thermal velocity, U_i – ionization potential.

For electrons we can use hydrodynamic model and to solve system (1)–(6), where instead Eq. (2) and (5), the equations are used:

$$j_i = \int v_i f_i dv \quad \text{and} \quad n_i = \int f_i dv \quad (17)$$

The numerical solution of the system of Eqs. (13)–(17) showed that in the stationary case the difference between two models is insignificant (see **Figure 9a**). A comparison between the results of both models obtained in model experiments testifies to an insignificant influence of the neutral component of a working gas on the formation of the potential drop across the discharge gap for the examined initial conditions.

To solve the Eqs. (13) and (14), we chose a time step that satisfies the condition $\Delta t < \Delta x/v_{imax}$, where Δx – spatial step, v_{imax} – maximal ion velocity. The **Figure 10** shows ion density changing in the gap during the time in high-current mode (under applied anode potential equal 1200 V). At first ions number increases in near anode region and remains almost constant in gap, then it increases almost linearly throughout the gap and finally increases sharply at the cathode region.

Note that for correct description (especially high-current mode), it is necessary to model ionization, collisions, and plasma creation, as well as motion of neutrals and formed ions in the whole volume of accelerator, thus need consider two-dimensional hybrid model.

3.1.3 2D-hybrid model and results

In the framework of this model the kinetic description is used in cylindrical geometry for the ionic and neutral components and the hydrodynamic

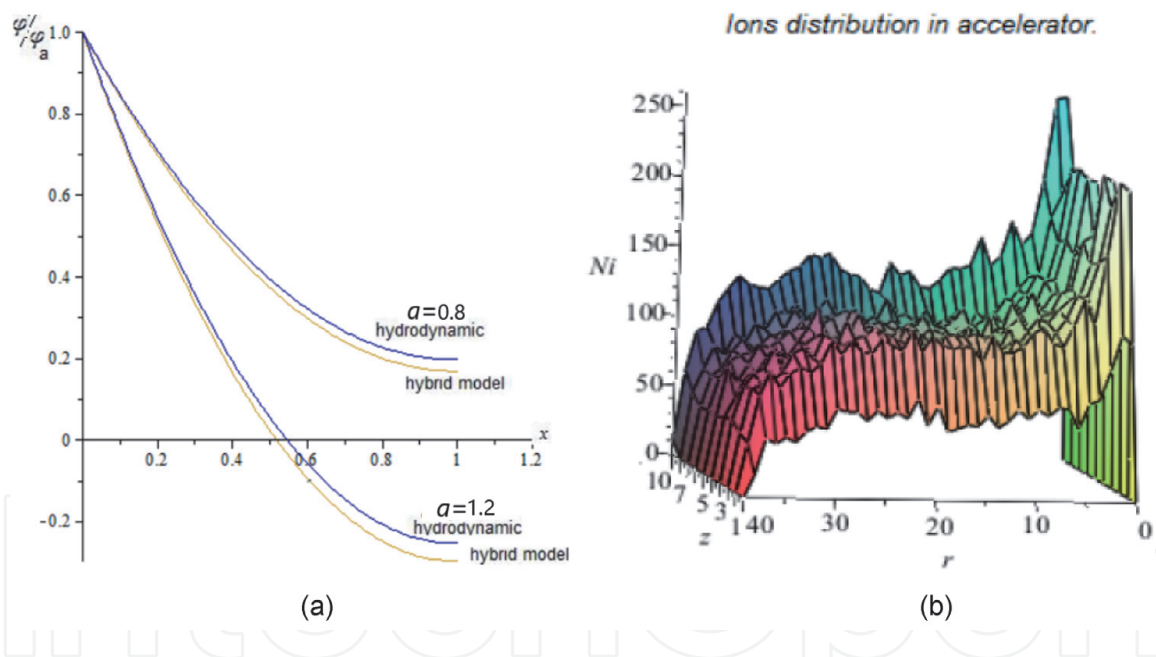


Figure 9. a) Comparison between the results of numerical calculations for the potential distribution in the discharge gap in the hydrodynamic and hybrid models. b) Ions number dependence on r and z ($r = 0, z = 0$ – center of the system).

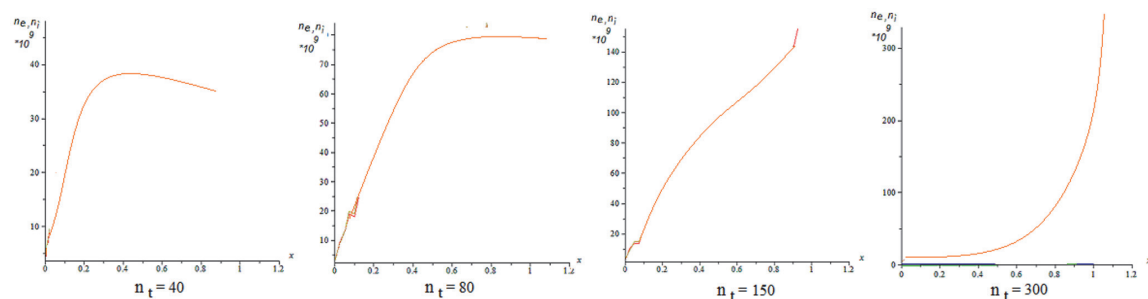


Figure 10. Ion distribution in the gap on different time steps.

one-dimension on each special layer $z_i < z < z_{i+1}$ description for the electron ones. Thus, for ions and neutrals description we use Boltzmann kinetic equation:

$$\frac{\partial f_{i,n}}{\partial t} + \vec{v}_{i,n} \frac{\partial f_{i,n}}{\partial \vec{r}} + \frac{e}{M} \left(E + \frac{1}{c} [\vec{v} \times B] \right) \frac{\partial f_i}{\partial v_i} = St \{ f_{i,n} \} \quad (18)$$

We solved this equation by splitting on the Vlasov equation for finding trajectories of ions and neutrals:

$$\frac{\partial f_{i,n}}{\partial t} + \vec{v}_{i,n} \frac{\partial f_{i,n}}{\partial \vec{r}} + \frac{e}{M} \left(E + \frac{1}{c} [\vec{v} \times B] \right) \frac{\partial f_i}{\partial v_i} = 0 \quad (19)$$

and to correct the found trajectories considering the collision integral, in which we took into account the processes of ionization and elastic and inelastic collisions:

$$\frac{Df_{i,n}}{Dt} = St \{ f_{i,n} \} \quad (20)$$

The Vlasov equations were solved by the method of characteristics [20]:

$$\frac{d\vec{v}_k}{dt} = \frac{q_k}{M} \left(\vec{E} + \frac{1}{c} [\vec{v}_k \times B] \right), \frac{d\vec{r}_k}{dt} = \vec{v}_k \quad (21)$$

To solve these equations the PIC method [21] with Boris scheme [22] was used to avoid singularities at the axis. For initial electric field distribution was taken electric field in the plasma absence: $E(r) = \frac{U_a}{r \ln(r_c/r_a)}$. The Monte-Carlo method was used for modeling of ionization in this field. The probability of a collision of a particle with energy ε_j during time Δt was found from expression [23]:

$$P_j = 1 - \exp \left(-v_j \Delta t \sigma(\varepsilon_j) n_j(\vec{r}_j) \right) \quad (22)$$

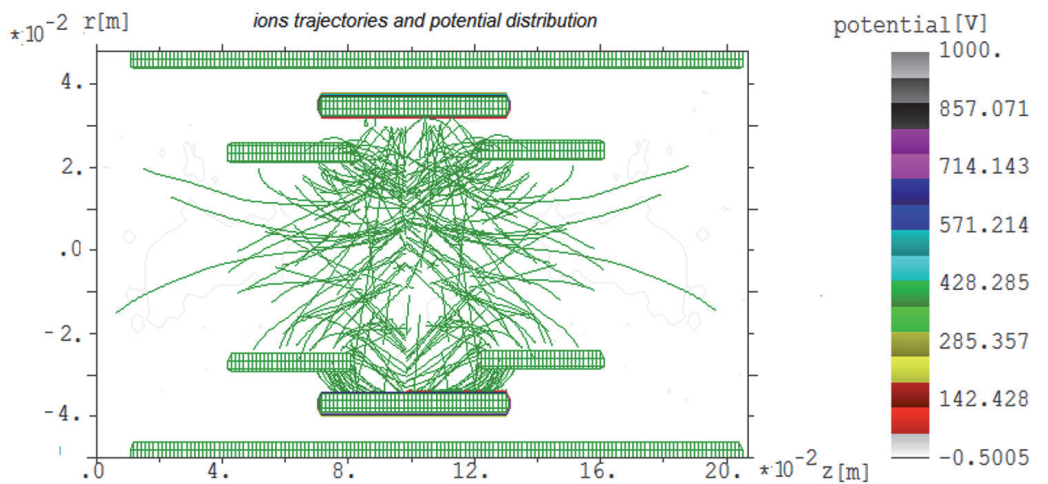
here $\sigma(\varepsilon)$ – collision cross-section (elastic, ionization or excitation), n_j – density of similar particles at the point r_j . To determine the probability of collision a random number s is chosen from interval $[0, 1]$ with the help of a random number generator. If $s < P_j$, then assumed that collision has occurred. It is determined by the ratio of the cross-sections with the random number generator, which collision has occurred – elastic, excitation, or ionization. In dependence of this particle parameters change or new ion add in computational box. The evolution of all particles that are in the modeling region is traced at each time step. For this motion equations were solved, and new velocities and positions of the particles were found. Particles that move out the modeling box boundaries are excluded from consideration. After quite a long time particle density distribution was found. The ion charge density and current density are calculated from coordinates and velocities particles according to formulas:

$$\rho(r, t) = \frac{1}{V} \sum_j q_j R(\vec{r}, \vec{r}_j(t)), j(r, t) = \sum_j q_j v_j(t) R(\vec{r}, \vec{r}_j(t)) \quad (23)$$

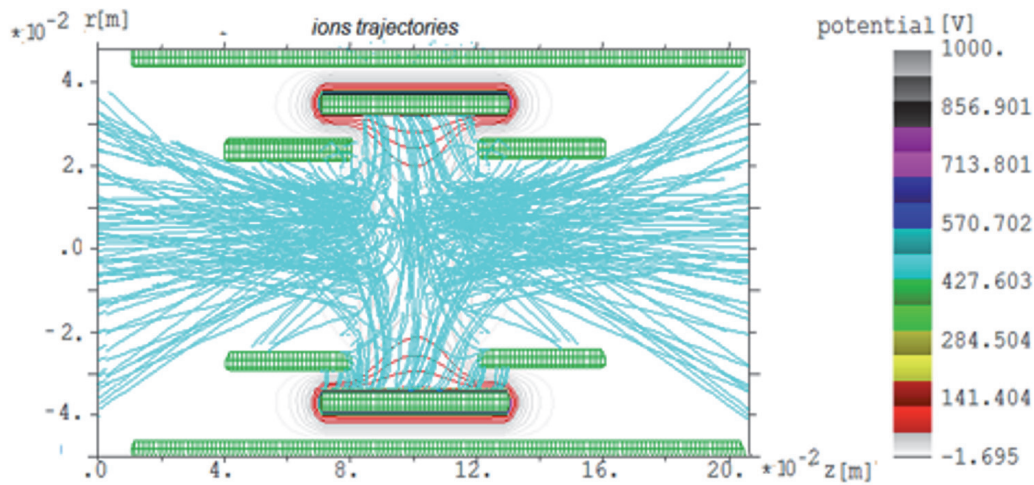
where $R(r, r_j)$ – usual standard PIC – core, that characterizes particle size and shape and charge distribution in it. For a cylindrical coordinate system it has form [24]:

$$R((r_1, z_k), (r_j, z_j)) = \begin{cases} \frac{1}{V_i} * \frac{r_{i+1}^2 - r_j^2}{r_{i+1}^2 - r_i^2} * \frac{h_z - |z_k - z_j|}{h_z}, & r_i < r_j < r_{i+1}, |z_k - z_j| < h_z \\ \frac{1}{V_i} * \frac{r_{i-1}^2 - r_j^2}{r_{i-1}^2 - r_i^2} * \frac{h_z - |z_k - z_j|}{h_z}, & r_{i-1} < r_i < r_{i+1}, |z_k - z_j| < h_z \\ 0, & i \end{cases} \quad (24)$$

here $V_i = 2\pi r_i h_r h_z$ – volume of the cell, h_r , h_z – steps in the spatial coordinates. After that the Poisson equation was solved and new electric field distribution was found. Since electrons are magnetized, we consider their movement in radial plane only, thus can solve for electrons one-dimensional hydrodynamic equations on each layer at z separately. Solve it we find electron density, calculate electric field on each layer and correct particle trajectories. After that the procedure was repeated. Modeling time is large enough for establish of ion multiplication process. The formation of the sufficient number of ions is possible due to magnetic field presence, which isolates anode from the cathode. Ions practically do not feel the magnetic field action and move from anode to the axis, where create a space charge, first in the center of the system. Electrons move along the magnetic field strength



(a)

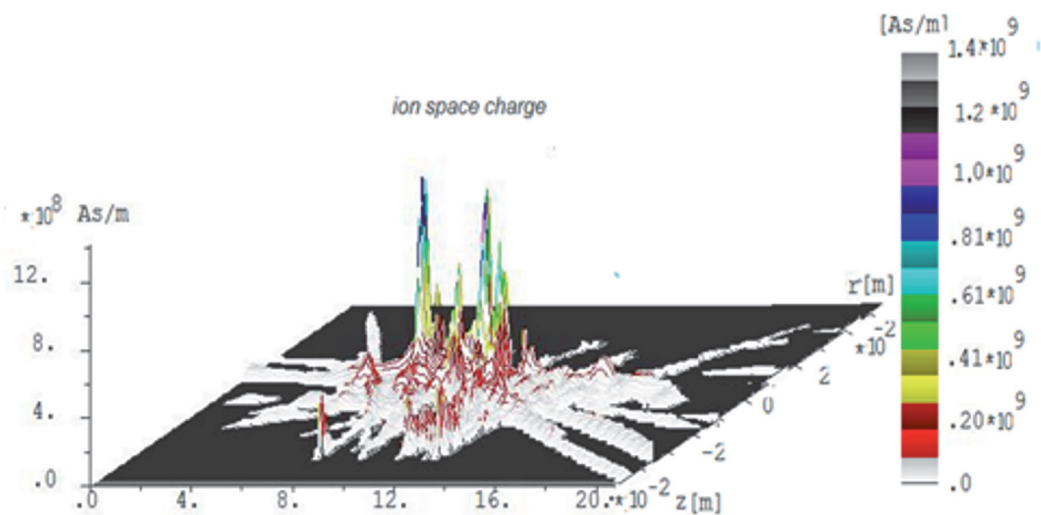


(b)

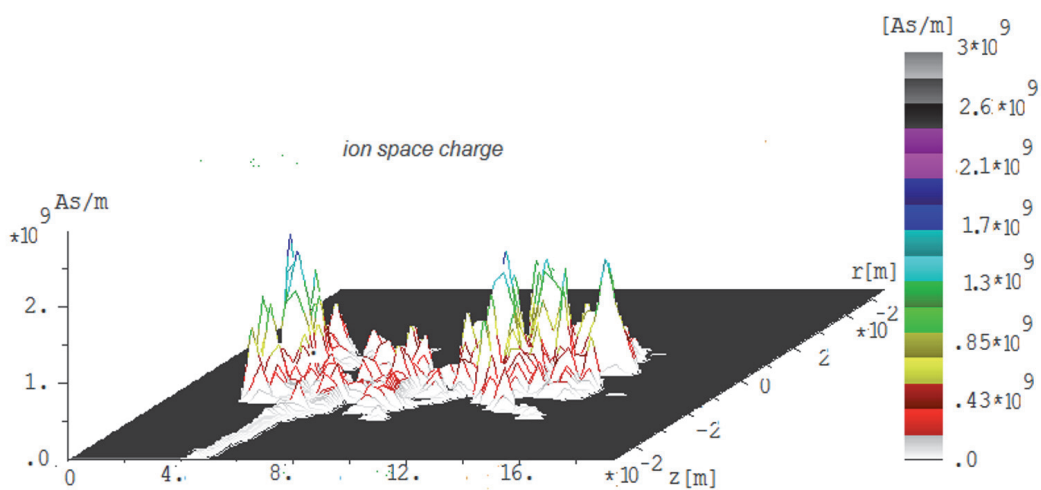
Figure 11. Ion's trajectories (calculation for $U_a = 1$ kV, $H = 0.03$ T) for different time step a) $N_t = 50$, b) $N_t = 200$.

line, but due to collisions with neutrals, they start move across the magnetic field. An internal electric field is formed which slow down the ions and pushes out them from the volume along system axis. The **Figure 9b** shows results of modeling high-current mode ($U_a = 1.2$ kV, pressure 0.15 Pa and magnetic field at the axis is 0.03 T). In is shown how the ions number to axis increases when ionization process is steady-state. One can see that number of ions increase not only to axis but along axis from center to edge too. In **Figure 11** the calculated ion trajectories for different time steps are shown. One can see that the ions that appear due to ionization move to center of the system. Coinciding on the system axis, they accumulate and create a positive space charge, and then diverge along the axis in both directions under the action of created own electric field. The ion space charge distribution for these case is shown in **Figure 12**.

The electrons trajectories for this case are shown in **Figure 13a**. One can see that the electrons are magnetized, moving along magnetic strength lines, and their trajectories are almost parallel to the surface of the anode. The **Figure 14** shows the potential distribution for different time steps. One can see that at the beginning of ionization, the potential drop is not complete in the gap and even has a negative sign in the center of the system. With ions number increasing, they coincide in the



(a)



(b)

Figure 12.
 Ion space charge for time step 70 (a) and 340 (b).

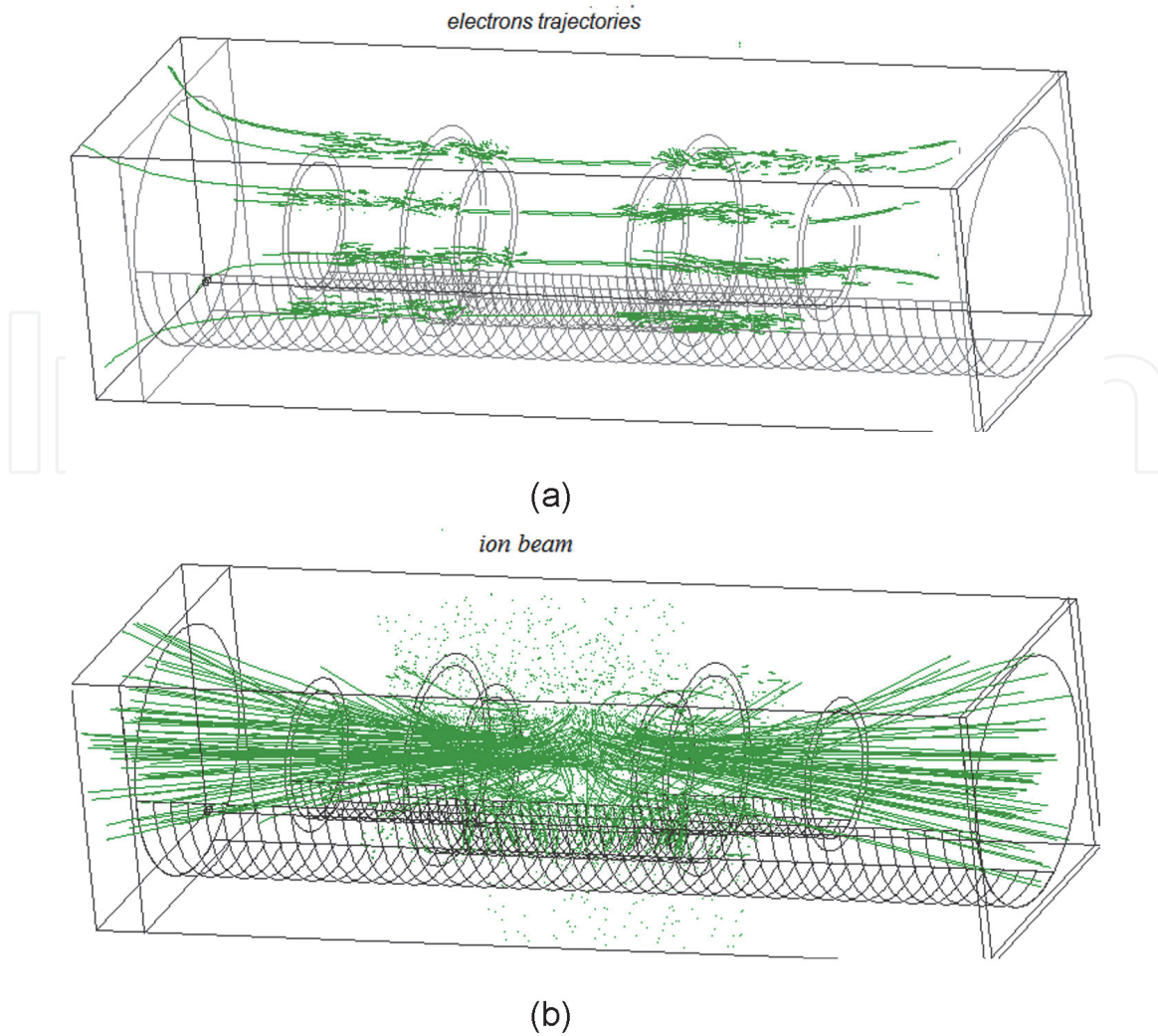


Figure 13. Electron (a) and ions (b) trajectories in accelerator for $H = 0.03$ T.

center of the system and form a positive space charge cloud, the potential of which even exceeds the applied potential U_a . This creates an electric field under which ions begin to move along the axis of symmetry in both directions, from the center to the edges, taking out with them part of space charge, reducing it in the center and creating bulks of space charge at the ends of the system (see **Figure 12**).

If we look at the potential distribution along the z -axis, we see that the maximum potential with distance from the center first declines, but then gradually begins to increase (see **Figure 15**). One can see that at a distance of 0.16 m from system center maximum potential is 222 V ($\sim 0.22 U_a$), while at a distance 0.21 m it is already 396 V, which is equal to $0.4 U_a$, and current density of ion beam reached 0.7 mA/cm^2 . Thus, the formed ions, initially accumulating in the center of the system, under action of own created electric field can accelerated and create a powerful ion flux from both edges of the accelerator.

4. Conclusion

Our research of the accelerator with closed electron drift and open walls demonstrates its similarity to the accelerator with anode layer and metallic walls in the accelerator channel. The low-current operation mode with an anode layer confined by the interelectrode gap and the high-current operation mode with

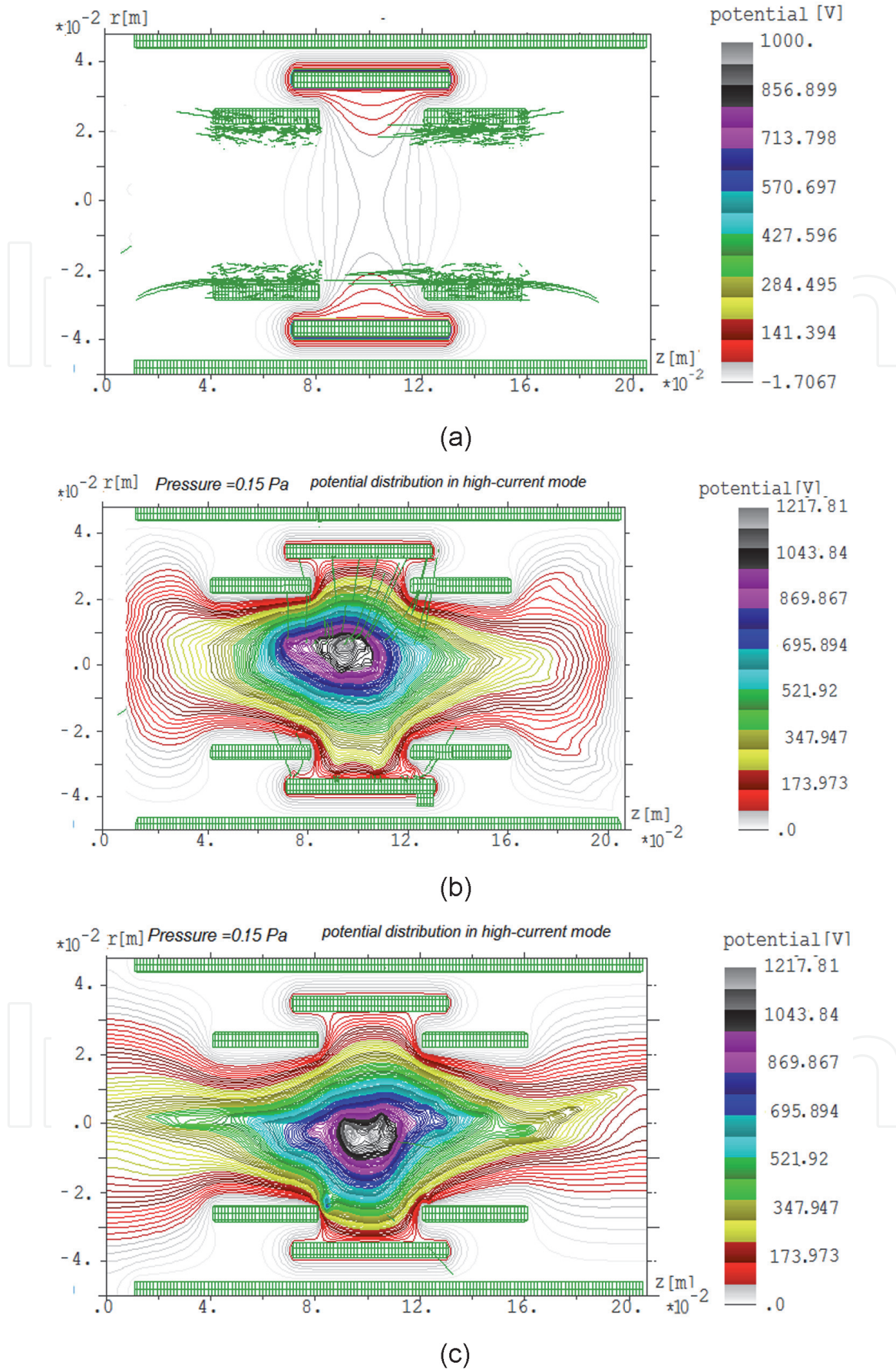


Figure 14.
 Potential distribution for different time step: a) $N_t = 10$, b) $N_t = 100$, c) $N_t = 300$.

well-distinguishable plasma torches at system's ends are obtained. The jump-like transition between the modes is shown to occur under the influence of the anode potential and the working gas pressure. In the low-current mode, the discharge

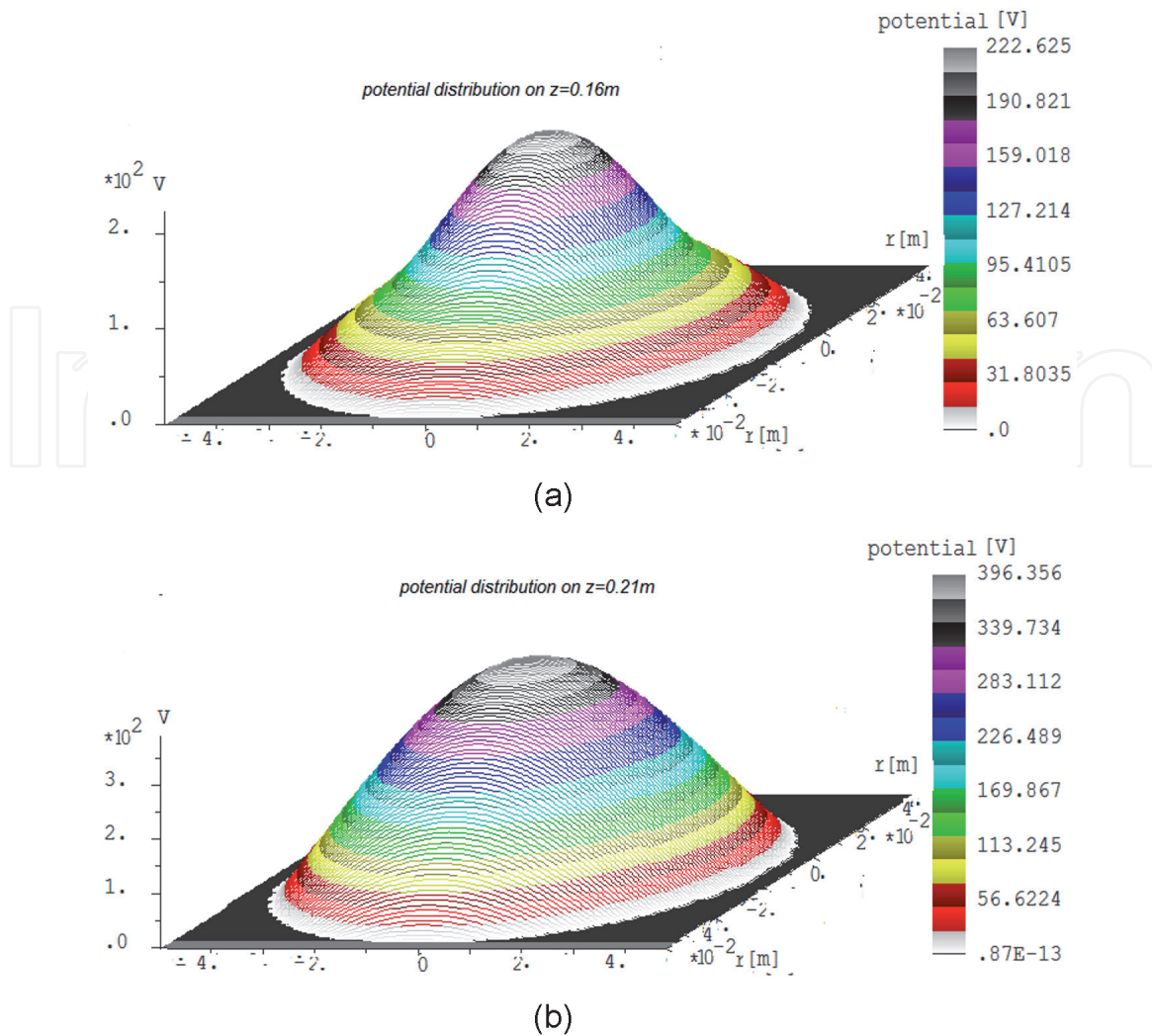


Figure 15. Potential distribution on the system axis at different distances from the center of the system: a) $z = 0.16$ m., b) $z = 0.22$ m.

current depends much stronger on the voltage applied across the discharge gap than on the working gas pressure. A hybrid theoretical model was developed, and simulation results on its basis are obtained. In the framework of this model the possibility of creation a positive space charge at the system axes is shown. It is shown that the ions flow from the hump of electrical potential can lead to the creation of a powerful ion flow, which moves along the symmetry axis in both sides from the center.

Thus, it is shown the carried out theoretical and experimental explorations demonstrate attractive perspective for further development and elaboration new generation erosion-free Hall-type accelerators. This open up possibility to apply kind improved devices like the space electric propulsions and tools for High-Tech ion-plasma surface treatment of functional materials.

Acknowledgements

The work was performed within the framework of the targeted comprehensive program "Prospective research in the field of plasma physics, controlled fusion and plasma technologies" under the project PL-2021.

IntechOpen

IntechOpen

Author details

Iryna Litovko^{1*}, Alexey Goncharov², Andrew Dobrovolskyi² and Iryna Naiko²

1 Institute for Nuclear Research NAS of Ukraine, Kiev, Ukraine

2 Institute of Physics NASU, Kiev, Ukraine

*Address all correspondence to: ilitovko@ukr.net

IntechOpen

© 2021 The Author(s). Licensee IntechOpen. This chapter is distributed under the terms of the Creative Commons Attribution License (<http://creativecommons.org/licenses/by/3.0>), which permits unrestricted use, distribution, and reproduction in any medium, provided the original work is properly cited. 

References

- [1] Morozov A. and Lebedev S.; “Plasmaoptics” in *Reviews of Plasma Physics*, Edited by M. Leontovich (Consultants Bureau, New York, 1975).
- [2] Grishin D., Leskov L., Kozlov N., *Plasma Accelerators*, Mashinostroenie (1983), Moscow-231 c.
- [3] Kim V.P. Design features and peculiarities of working processes in modern stationary plasma engines of Morozov (in Russian). *Journal of Technical Physics*, 2015, v. 85, #3, pp. 45-59.
- [4] Choueiri E. Y. A Critical History of Electric Propulsion: The First 50 Years (1906–1956). *Journal of propulsion and power*, Vol. 20, No. 2, March–April 2004
- [5] Ding Y., Peng W., Sun H., Wei L., Zeng M., Wang F., and Yu D., “Performance characteristics of no-wall-losses hall thruster,” *Eur. Phys. J. Spec. Top.* 226, 2945 (2017).
- [6] Mazouffre, S., Vaudolon, J., Tsikata, S., et al. “Optimization of magnetic field topology and anode geometry for a Wallless hall Thruster,” 51st AIAA/SAE/ASEE Joint Propulsion Conference, AIAA2015–4007, Cleveland, Ohio, 2015
- [7] Goncharov A., Dobrovolsky A., Litovko I., Naiko I., Naiko L. Plasma accelerator with closed electron drift and open walls. *Problems of atomic science and technology*. – 2015. – №4 (98). – P. 26-31.
- [8] Litovko I., Goncharov A., Dobrovolskiy A., Naiko L., Naiko I. Computer modelling new generation plasma optical devices (new results) *Problems of atomic science and technology*. – 2015. – №1(95). – P. 209-212.
- [9] Goncharov A.A., Dobrovolskiy A.N., Litovko I.V., Naiko I.V., Naiko L.V. Modes of plasma-dynamical system with closed electron drift and open wall. 2017 IEEE International young scientists forum on applied physics and engineering (YSF-2017). Book of papers. – 2017. – P. 267-270. DOI: 10.1109/YSF.2017.8126633
- [10] Goncharov A., Dobrovolsky A., Litovko I., Naiko L., Naiko I Novel modification of Hall-type ion source (study and the first results). *Rev. Sci. Instrum.* – 2016. – P. 87, 02A501.
- [11] Morozov A. I. *Intrduction in Plasmodynamics* (CRC Press, 2012); (in Russian: – M.: Fismatlit, 2006.) – 576 p.
- [12] Goncharov A.A., Dobrovolskiy A. N., Evsyukov A.N., Protsenko I.M., Litovko I.V. New vision of the physics of gas magnetron-type discharges. *Ukr. J. Phys*, 2009, vol. 54, №1-2, pp. 63-67
- [13] *Physics and Applications of Plasma Accelerators*, edited by A.I. Morozov. – Minsk: Nauka i tehnika, 1974.
- [14] Goncharov A. A., Dobrovolskiy A. M., Dunets S. M., Litovko I. V., Gushenets V. I. et al. Electrostatic plasma lens for focusing negatively charged particle beams. *Rev. Sci. Instrum.* 83, 02B723 (2012); doi: 10.1063/1.3675387
- [15] Goncharov, A. Dobrovolskiy, S. Dunets, A. Evsyukov, I. Litovko, V. Gushenets, E. Oks., Positive-Space-Charge Lens for Focusing and Manipulating High-Current Beams of Negatively Charged Particles. *IEEE Trans. Plasma Sci.*, v. 39, № 6 (2011), pp. 1408-141113
- [16] V. Gushenets, A. Goncharov, A. Dobrovolskiy, S. Dunets, I. Litovko, E. Oks., A. Bugaev, Electrostatic plasma lens focusing of an intense electron beam in an electron source with a vacuum arc plasma cathode. *IEEE*

Trans. Plasma Sci., v. 41, № 4, Part 3
(2013), pp. 2171-2174

[17] Goncharov, A. Dobrovolskiy, I. Litovko, V. Gushenets, E. Oks. Focusing intense electron beams using a positive space charge cloud plasma lens. *Physica Scripta*, v. 161, 014070 (2014).

[18] Litovko I.V., Dobrovolskiy A.N., Naiko L.V., Naiko I.V. a new type of plasma accelerator with closed electron drift. *Ukr. J. Phys.* 2018. Vol. 63, No. 2. Pp. 110–115.

[19] Litovko I.V., Goncharov A.A., Dobrovolskiy A.N., Naiko L.V., Naiko I. V., Modelling of new generation plasma optical devices//*Nukleika*, 2016, vol. 61 (2), pp. 207-212.

[20] Pegoraro F. Theory and applications of the Vlasov equation. /F. Pegoraro, F. Califano, G. Manfredi, P. J. Morrison/ *Eur. Phys. J. D.* — 2015. — Vol. 69.— P. 68. — DOI:10.1140

[21] Potter D. *Methods of Calculations in Physics* (Mir, Moscow, 1975)

[22] Boris J.P., Lee R. Optimization of particle calculations in 2 and 3 dimensions, *Commun. Math. Phys.* 1969. № 12. p. 131

[23] V. Vahedi, M. Surendra, “A Monte Carlo collision model for the particle-in-cell method: Application for argon and oxygen discharges»//*Computer Physics Communications* 87 (1995), 179-198

[24] Birdsall C.K. Particle-in-Cell charged-particle simulation plus Monte Carlo collisions with neutral atoms, PIC-MCC/C.K. Birdsall//*IEEE Transactions on Plasma Science.* – 1991. – Vol. 19. – № 2. – P. 65-83.